

Overview of \bar{K} -Nuclear Quasi-Bound States*

Avraham Gal^a

^aRacah Institute of Physics, The Hebrew University, Jerusalem 91904, Israel

Experimental evidence for \bar{K} -nuclear quasi-bound states is briefly reviewed. Theoretical and phenomenological arguments for and against the existence of such states are considered, based on constructing \bar{K} -nuclear optical potentials from various sources. Results of RMF calculations that provide a lower limit of $\Gamma_{\bar{K}} \sim 50 \pm 10$ MeV on the width of \bar{K} -nuclear quasi-bound states are discussed.

1. INTRODUCTION

The \bar{K} -nucleus interaction near threshold is strongly attractive and absorptive as suggested by fits to the strong-interaction shifts and widths of K^- -atom levels [1]. Global fits yield ‘deep’ optical potentials with $\text{Re } V_{\bar{K}}(\rho_0) \sim -(150 - 200)$ MeV [2–5], whereas more theoretically inclined studies that fit the low-energy K^-p reaction data, including the $I = 0$ quasi-bound state $\Lambda(1405)$ as input for constructing density dependent optical potentials, suggest relatively ‘shallow’ potentials with $\text{Re } V_{\bar{K}}(\rho_0) \sim -(40 - 60)$ MeV [6–8]. The issue of depth of the attractive \bar{K} -nucleus potential is discussed in Section 2.

Paradoxically, due to the strong (absorptive) $\text{Im } V_{\bar{K}}$, relatively narrow K^- deeply bound *atomic* states are expected to exist [9], independently of the size of $\text{Re } V_{\bar{K}}$. Figure 1 from Ref. [10] shows on the left-hand side a calculated spectrum of K^- atomic states in ^{208}Pb where, in particular, all the circular states below the $7i$ ($l = 6$) state are not populated by X-ray transitions due to the strong K^- -nuclear absorption, and on the right-hand side it demonstrates saturation of the $2p$ atomic-state width as a function of the absorptivity parameter $\text{Im } b_0$ of $V_{\bar{K}}$. The physics behind is that a strong $\text{Im } V_{\bar{K}}$ acts repulsively, suppressing the *atomic* wavefunction in the region of overlap with $\text{Im } V_{\bar{K}}$. The calculated width of the ‘deeply bound’ atomic $1s$ and $2p$ is less than 2 MeV, also confirmed by the calculation of Ref. [11], calling for experimental ingenuity how to form these levels selectively by a non-radiative process [12].

This saturation mechanism does not hold for \bar{K} -nuclear states which retain very good overlap with the potential. Hence, the questions to ask are (i) whether it is possible at all to bind *strongly* \bar{K} mesons in nuclei, and (ii) are such quasi-bound states sufficiently narrow to allow observation and identification? The first question was answered favorably by Nogami [13] as early as 1963 arguing that the K^-pp system could acquire about 10 MeV binding in its $I = 1/2$ state. Yamazaki and Akaishi, within a single-channel K^-pp calculation [14], reported a binding energy $B \sim 50$ MeV and width $\Gamma \sim 60$ MeV; however,

*Plenary talk given at Few-Body 18, Santos, Brazil, August 2006, to be published in Nucl. Phys. A

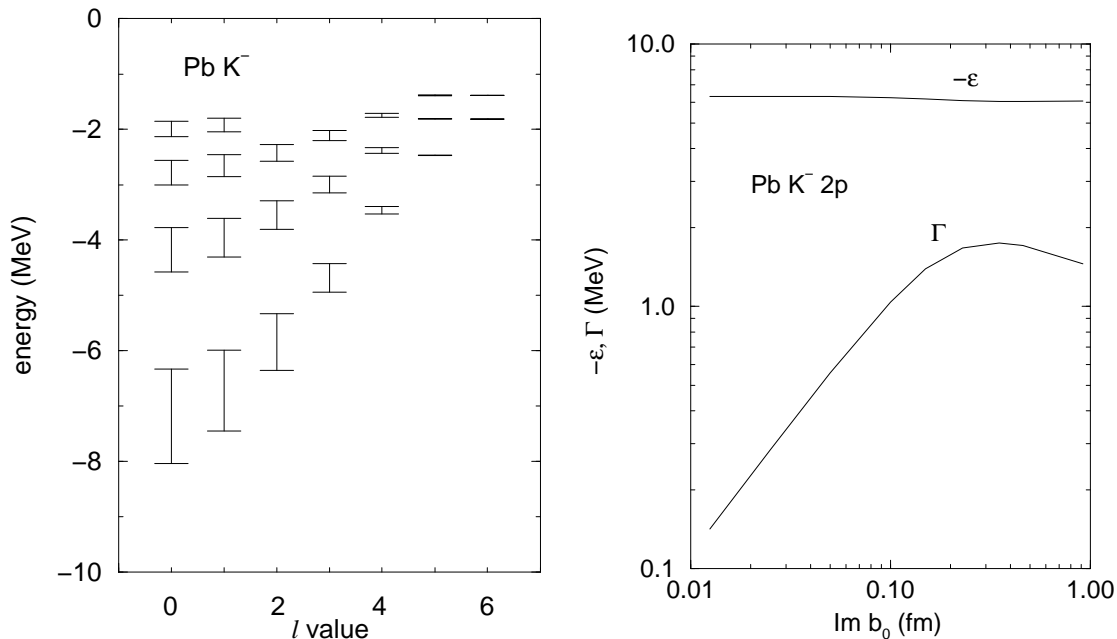


Figure 1. Left: calculated K^- ‘deeply bound’ atomic states in ^{208}Pb . Right: saturation of width Γ for the $2p$ K^- - ^{208}Pb atomic state as function of $\text{Im } b_0$, for $\text{Re } b_0 = 0.62$ fm.

the recent coupled-channel $\bar{K}NN - \pi\Sigma N$ Faddeev calculation for K^-pp by Shevchenko et al. [15] finds a substantially broader $I = 1/2$ state ($B \sim 60$ MeV, $\Gamma \sim 100$ MeV).

The current experimental and theoretical interest in \bar{K} -nuclear bound states was triggered back in 1999 by the suggestion of Kishimoto [16] to look for such states in the nuclear reaction (K^-, p) in flight, and by Akaishi and Yamazaki [17,18] who suggested to look for a $\bar{K}NNN$ $I = 0$ state bound by over 100 MeV for which the main $\bar{K}N \rightarrow \pi\Sigma$ decay channel would be kinematically closed.² Some controversial evidence for relatively narrow states was presented initially in (K_{stop}^-, n) and (K_{stop}^-, p) reactions on ^4He (KEK-PS E471) [20,21] but has just been withdrawn (KEK-PS E549/570) [22]. \bar{K} -nuclear states were also invoked to explain few weak irregularities in the neutron spectrum of the (K^-, n) in-flight reaction on ^{16}O (BNL-AGS, parasite E930 [23]), but subsequent (K^-, n) and (K^-, p) reactions on ^{12}C at $p_{\text{lab}} = 1$ GeV/c (KEK-PS E548 [24]) have not disclosed any peaks beyond the appreciable strength observed below the \bar{K} -nucleus threshold. Ongoing experiments by the FINUDA spectrometer collaboration at DAΦNE, Frascati, already claimed evidence for a relatively broad K^-pp deeply bound state ($B \sim 115$ MeV) in K_{stop}^- reactions on Li and ^{12}C , by observing back-to-back Λp pairs from the decay $K^-pp \rightarrow \Lambda p$ [25], but these pairs could more naturally arise from conventional absorption processes at rest when final-state interaction is taken into account [26]. Indeed, the $K_{\text{stop}}^-pn \rightarrow \Sigma^-p$ reaction on ^6Li has also been recently observed [27]. Another recent claim for a very narrow and deep K^-pp state ($B \sim 160$ MeV, $\Gamma \sim 30$ MeV) is also based on observing decay Λp pairs, using \bar{p}

²Wycech had conjectured that the width of such states could be as small as 20 MeV [19].

annihilation data on ${}^4\text{He}$ from the OBELIX spectrometer at LEAR, CERN [28]. One cannot rule out that the Λp pairs assigned in the above analyses to K^-pp decay in fact result from nonmesonic decays of different clusters, say the $\bar{K}NNN$ $I = 0$ quasi-bound state. A definitive identification may only be reached through a fully exclusive formation analysis, such as the one scheduled for J-PARC [29]:

$$K^- + {}^3\text{He} \rightarrow (K^-pp) + n. \quad (1)$$

Finally, preliminary evidence for the $\bar{K}NNN$ $I = 0$ state ($B \sim 50-60$ MeV, $\Gamma \sim 35$ MeV) has been recently presented by the FINUDA collaboration on ${}^6\text{Li}$ by observing back-to-back Λd pairs [30]. It is clear that the issue of \bar{K} nuclear states is far yet from being experimentally resolved and more dedicated, systematic searches are necessary.

It is interesting then to study theoretically \bar{K} nuclear quasi-bound states in the range of binding energy $B_{\bar{K}} \sim 100 - 200$ MeV, in particular the width anticipated for such deeply bound states. This is described in Section 3 within the relativistic mean field (RMF) model for a system of nucleons and one \bar{K} meson interacting through the exchange of scalar (σ) and vector (ω, ρ) boson fields which are treated in the mean-field approximation [5,31].

2. \bar{K} -NUCLEUS POTENTIALS

2.1. Chirally motivated models

The Born approximation for $V_{\bar{K}}$ due to the leading-order Tomozawa-Weinberg (TW) vector term of the chiral effective Lagrangian [32] yields a sizable attraction:

$$V_{\bar{K}} = -\frac{3}{8f_\pi^2} \rho \sim -55 \frac{\rho}{\rho_0} \text{ MeV} \quad (2)$$

for $\rho_0 = 0.16 \text{ fm}^{-3}$, where $f_\pi \sim 93$ MeV is the pseudoscalar meson decay constant. Iterating the TW term plus next-to-leading-order terms, within an *in-medium* coupled-channel approach constrained by the $\bar{K}N - \pi\Sigma - \pi\Lambda$ data near the $\bar{K}N$ threshold, roughly doubles this \bar{K} -nucleus attraction. It is found (e.g. Ref. [33]) that the $\Lambda(1405)$ quickly dissolves in the nuclear medium at low density, so that the repulsive free-space scattering length a_{K-p} , as function of ρ , becomes *attractive* well below ρ_0 . Since the attractive $I = 1$ a_{K-n} is only weakly density dependent, the resulting in-medium $\bar{K}N$ isoscalar scattering length $b_0(\rho) = \frac{1}{2}(a_{K-p}(\rho) + a_{K-n}(\rho))$ translates into a strongly attractive $V_{\bar{K}}$:

$$V_{\bar{K}}(r) = -\frac{2\pi}{\mu_{KN}} b_0(\rho) \rho(r), \quad \text{Re } V_{\bar{K}}(\rho_0) \sim -110 \text{ MeV}. \quad (3)$$

However, when $V_{\bar{K}}$ is calculated *self consistently*, namely by including $V_{\bar{K}}$ in the propagator G_0 used in the Lippmann-Schwinger equation determining $b_0(\rho)$, one obtains $\text{Re } V_{\bar{K}}(\rho_0) \sim -(40 - 60)$ MeV [6-8]. The main reason for this weakening of $V_{\bar{K}}$, approximately back to that of Eq. (2), is the strong absorptive effect which $V_{\bar{K}}$ exerts within G_0 to suppress the higher Born terms of the $\bar{K}N$ TW potential.

2.2. Fits to K^- -atom data

The K^- -atom data used in global fits [1] span a range of nuclei from ${}^7\text{Li}$ to ${}^{238}\text{U}$, with 65 level-shift and -width data points. Figure 2 shows fitted \bar{K} -nucleus potentials for ${}^{58}\text{Ni}$

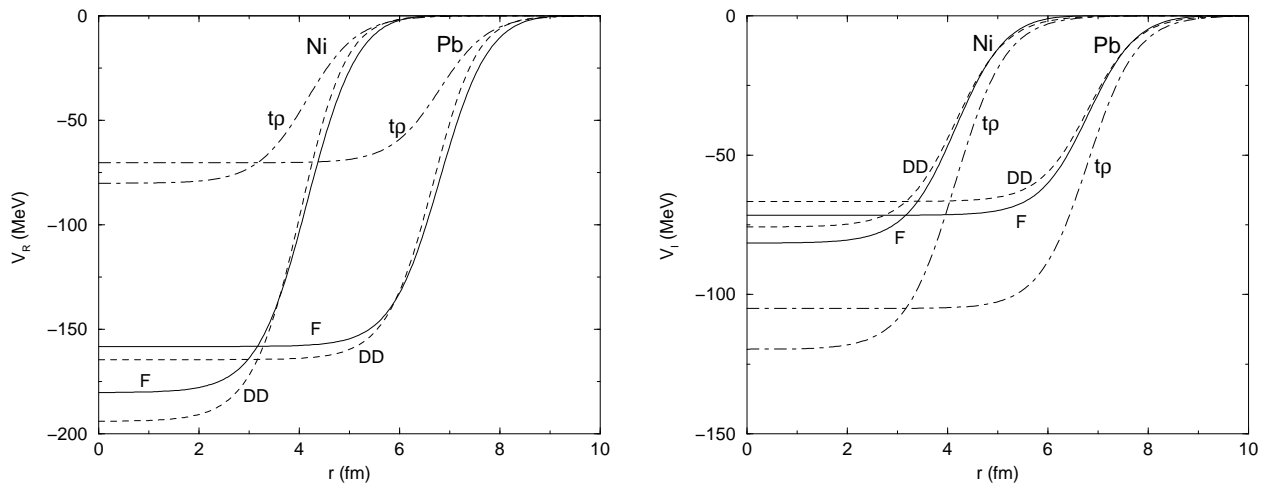


Figure 2. Real part (left) and imaginary part (right) of the \bar{K} -nucleus potential for ^{58}Ni and ^{208}Pb , obtained in a global fit to K^- -atom data, for a $t\rho$ potential, for the DD potential [1] and for potential F [5], see text.

and ^{208}Pb , for a $t\rho$ potential with a complex strength t , and for two density-dependent potentials marked by DD and F, also fitted to the same data. For the real part, the depth of the $t\rho$ potential is about 70 – 80 MeV, whereas the density-dependent potentials are considerably deeper, 150 – 200 MeV. These latter potentials yield substantially lower χ^2 values of 103 and 84, respectively, than the value 129 for the $t\rho$ potential. We note that, although the two density-dependent potentials have very different parameterizations, the resulting potentials are quite similar. In particular, the shape of potential F departs appreciably from $\rho(r)$ for $\rho(r)/\rho_0 \leq 0.2$, where the physics of the $\Lambda(1405)$ still plays some role. The density dependence of the potential F is qualitatively similar to that of Eq. (3), by far providing the best fit ever reported for a global K^- -atom data fit.

2.3. Further considerations

Additional considerations for estimating $V_{\bar{K}}$ are listed below.

(i) QCD sum-rule estimates [34] for vector (v) and scalar (s) self-energies:

$$\Sigma_v(\bar{K}) \sim -\frac{1}{2} \Sigma_v(N) \sim -\frac{1}{2} (200) \text{ MeV} = -100 \text{ MeV}, \quad (4)$$

$$\Sigma_s(\bar{K}) \sim \frac{m_s}{M_N} \Sigma_s(N) \sim \frac{1}{6} (-300) \text{ MeV} = -50 \text{ MeV}, \quad (5)$$

where m_s is the strange-quark (current) mass. The factor 1/2 in Eq. (4) is due to the one nonstrange antiquark in the \bar{K} out of two possible, and the minus sign is due to G -parity going from quarks to antiquarks. This rough estimate gives then $V_{\bar{K}}(\rho_0) \sim -150$ MeV. The QCD sum-rule approach essentially refines the mean-field argument [35,36]

$$V_{\bar{K}}(\rho_0) \sim \frac{1}{3} (\Sigma_s(N) - \Sigma_v(N)) \sim -170 \text{ MeV}, \quad (6)$$

where the $1/3$ factor is again due to the one nonstrange antiquark in the \bar{K} , but here with respect to the three nonstrange quarks of the nucleon.

(ii) The ratio of K^-/K^+ production cross sections in nucleus-nucleus and proton-nucleus collisions near threshold, measured by the Kaon spectrometer (KaoS) at SIS, GSI, gives clear evidence for attractive $V_{\bar{K}}$, estimated [37] as $V_{\bar{K}}(\rho_0) \sim -80$ MeV by relying on BUU transport calculations normalized to the value $V_K(\rho_0) \sim +25$ MeV. Since the BUU calculations apparently disregard $\bar{K}NN \rightarrow YN$ absorption, a deeper $V_{\bar{K}}$ may follow when nonmesonic absorption is included.

3. RMF DYNAMICAL CALCULATIONS

3.1. \bar{K} -nucleus RMF methodology

In this model, expanded in Ref. [5], the (anti)kaon interaction with the nuclear medium is incorporated by adding to \mathcal{L}_N the Lagrangian density \mathcal{L}_K :

$$\mathcal{L}_K = \mathcal{D}_\mu^* \bar{K} \mathcal{D}^\mu K - m_K^2 \bar{K} K - g_{\sigma K} m_K \sigma \bar{K} K . \quad (7)$$

The covariant derivative $\mathcal{D}_\mu = \partial_\mu + ig_{\omega K} \omega_\mu$ describes the coupling of the (anti)kaon to the vector meson ω . The coupling of the (anti)kaon to the isovector ρ meson was neglected, a good approximation for the light $N = Z$ nuclei. The \bar{K} meson induces additional source terms in the equations of motion for the meson fields σ and ω_0 . It thus affects the scalar $S = g_{\sigma N} \sigma$ and the vector $V = g_{\omega N} \omega_0$ potentials which enter the Dirac equation for nucleons, and this leads to rearrangement or polarization of the nuclear core. Furthermore, in the Klein-Gordon equation satisfied by the \bar{K} , the scalar $S = g_{\sigma K} \sigma$ and the vector $V = -g_{\omega K} \omega_0$ potentials become *state dependent* through the *dynamical* density dependence of the mean-field potentials S and V , as expected from a RMF calculation. The \bar{K} potential was made complex by adding $\text{Im } V_{\text{opt}}$ in a $t\rho$ form fitted to the K^- atomic data [4]. From phase-space considerations, $\text{Im } V_{\text{opt}}$ was then multiplied by a suppression factor, taking into account the binding energy of the antikaon for the initial decaying state, and assuming two-body final-state kinematics for the decay products in the $\bar{K}N \rightarrow \pi Y$ mesonic modes and in the $\bar{K}NN \rightarrow YN$ nonmesonic modes.

The coupled system of equations was solved self-consistently. To give rough idea, whereas the static calculation gave $B_{K^-} = 132$ MeV for the K^- $1s$ state in ^{12}C , using the values $g_{\omega K}^{\text{atom}}$, $g_{\sigma K}^{\text{atom}}$ corresponding to the K^- -atom fit, the dynamical calculation gave $B_{K^-} = 172$ MeV for this same state. In order to produce different values of binding energies, $g_{\sigma K}$ and $g_{\omega K}$ were varied in given intervals of physical interest.

3.2. Binding energies and widths

Beginning approximately with ^{12}C , the following conclusions may be drawn:

(i) For given values of $g_{\sigma K}$, $g_{\omega K}$, the \bar{K} binding energy $B_{\bar{K}}$ saturates, except for a small increase due to the Coulomb energy (for K^-).

(ii) The difference between the binding energies calculated dynamically and statically, $B_{\bar{K}}^{\text{dyn}} - B_{\bar{K}}^{\text{stat}}$, is substantial in light nuclei, increasing with $B_{\bar{K}}$ for a given value of A , and decreasing monotonically with A for a given value of $B_{\bar{K}}$. It may be neglected only for very heavy nuclei. The same holds for the nuclear rearrangement energy $B_{\bar{K}}^{\text{s.p.}} - B_{\bar{K}}$ which is a fraction of $B_{\bar{K}}^{\text{dyn}} - B_{\bar{K}}^{\text{stat}}$.

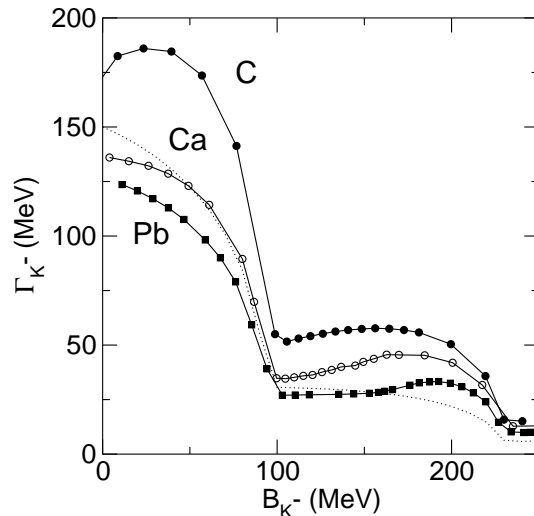


Figure 3. Dynamically calculated widths of the $1s$ K^- -nuclear state in ${}_{K^-}^{12}\text{C}$, ${}_{K^-}^{40}\text{Ca}$ and ${}_{K^-}^{208}\text{Pb}$ as function of the K^- binding energy for nonlinear RMF models. The dotted line is for a static nuclear-matter calculation with $\rho_0 = 0.16 \text{ fm}^{-3}$, see text.

(iii) The width $\Gamma_{\bar{K}}(B_{\bar{K}})$ decreases monotonically with A , according to Fig. 3 which shows calculated widths Γ_{K^-} as function of the binding energy B_{K^-} for $1s$ states in ${}_{K^-}^{12}\text{C}$ and ${}_{K^-}^{40}\text{Ca}$, using the nonlinear NL-SH version [38] of the RMF model, and in ${}_{K^-}^{208}\text{Pb}$ using the NL-TM1 version [39]. The dotted line shows the static ‘nuclear-matter’ limit corresponding to the K^- -atom fitted value $\text{Im } b_0 = 0.62 \text{ fm}$ and for $\rho(r) = \rho_0 = 0.16 \text{ fm}^{-3}$, using the same phase-space suppression factor as in the ‘dynamical’ calculations. It is clearly seen that the functional dependence $\Gamma_{K^-}(B_{K^-})$ follows the shape of the dotted line. This dependence is due primarily to the binding-energy dependence of the suppression factor f which falls off rapidly until $B_{K^-} \sim 100 \text{ MeV}$, where the dominant $\bar{K}N \rightarrow \pi\Sigma$ gets switched off, and then stays rather flat in the range $B_{K^-} \sim 100 - 200 \text{ MeV}$ where the width is dominated by the $\bar{K}NN \rightarrow YN$ absorption modes. The widths calculated in this range are considerably larger than given by the dotted line (except for Pb in the range $B_{K^-} \sim 100 - 150 \text{ MeV}$) due to the dynamical nature of the RMF calculation, whereby the nuclear density is increased by the polarization effect of the K^- . Adding perturbatively the residual width neglected in this calculation, partly due to the $\bar{K}N \rightarrow \pi\Lambda$ secondary mesonic decay channel, a representative value for a lower limit $\Gamma_{\bar{K}} \sim 50 \pm 10 \text{ MeV}$ holds in the binding energy range $B_{K^-} \sim 100 - 200 \text{ MeV}$.

3.3. Nuclear polarization effects

Figure 4 shows on the left-hand side the calculated average nuclear density $\bar{\rho} = \frac{1}{A} \int \rho^2 d\mathbf{r}$ as a function of B_{K^-} for K^- nuclear $1s$ states across the periodic table. In the light K^- nuclei, $\bar{\rho}$ increases substantially with B_{K^-} to values about 50% higher than without the \bar{K} . The increase of the central nuclear densities is even bigger, as demonstrated on the right-hand side for a family of $1s$ K^- states in ${}_{K^-}^{208}\text{Pb}$, but is confined to a small region

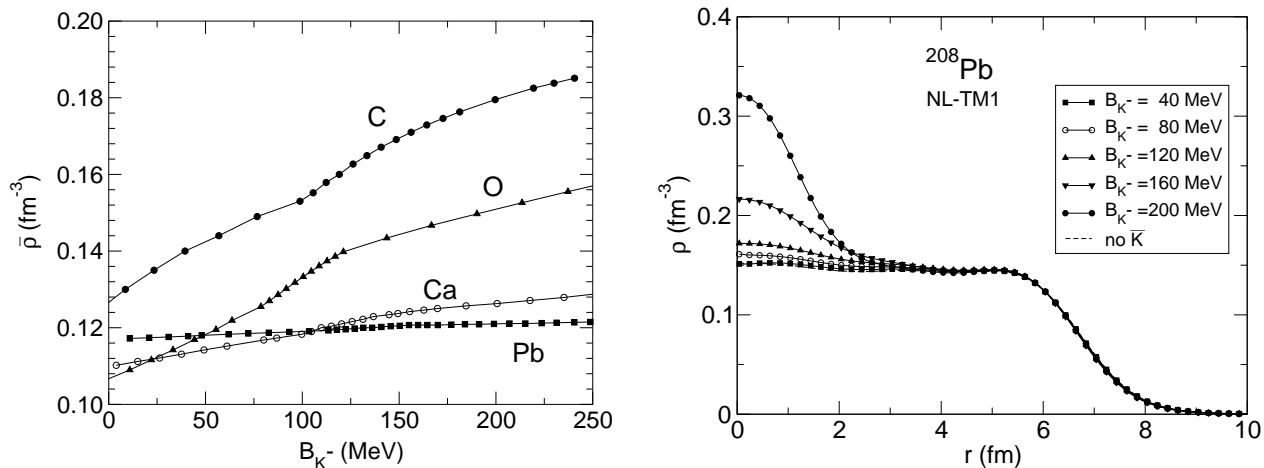


Figure 4. Calculated average nuclear density $\bar{\rho}$ for $^{12}_K\text{C}$, $^{16}_K\text{O}$, $^{40}_K\text{Ca}$ and $^{208}_K\text{Pb}$ (left) as function of $B_{K^-}(1s)$ for the NL-SH RMF model [38], and nuclear density ρ of $^{208}_K\text{Pb}$ (right) for several $B_{K^-}(1s)$ values, using the NL-TM1 RMF model [39].

subsiding almost completely by $r = 2$ fm, well within the nuclear volume. As a result, $\bar{\rho}(^{208}_K\text{Pb})$ on the left-hand side of Fig. 4 is only weakly enhanced as function of B_{K^-} .

4. CONCLUSIONS

In this talk I reviewed the phenomenological and theoretical evidence for a substantially attractive \bar{K}^- -nucleus interaction potential, from a ‘shallow’ potential of depth 40 – 60 MeV to a ‘deep’ potential of depth 150 – 200 MeV at nuclear-matter density. I then reported on recent *dynamical* calculations [5] for deeply quasi-bound K^- nuclear states across the periodic table. Substantial polarization of the core nucleus was found in light nuclei, but the ‘high’ densities reached are considerably lower than those found in the few-body calculations due to Akaishi, Yamazaki and collaborators [14,18,40,41]. An almost universal dependence of \bar{K}^- widths on the binding energy was found, for a given nucleus, reflecting the phase-space suppression factor on top of the increase provided by the density of the compressed nuclear core. The present results place a lower limit $\Gamma_{\bar{K}^-} \sim 50 \pm 10$ MeV which is particularly useful for \bar{K}^- binding energies exceeding 100 MeV.

ACKNOWLEDGMENTS

I wish to thank my collaborators Eli Friedman, Jiří Mareš and Nina Shevchenko, as well as Tullio Bressani, Evgeny Drukarev, Tomofumi Nagae and Wolfram Weise for stimulating discussions, and Lauro Tomio and the co-organizers of FB18 for their kind hospitality and support. Special thanks go to Wolfram Weise for his kind hospitality at the TU Munich where this report was prepared under the support of the Alexander von Humboldt Foundation. This work is supported in part by the Israel Science Foundation, Jerusalem, grant 757/05.

REFERENCES

1. C.J. Batty, E. Friedman, A. Gal, Phys. Rep. 287 (1997) 385.
2. E. Friedman, A. Gal, C.J. Batty, Phys. Lett. B 308 (1993) 6.
3. E. Friedman, A. Gal, C.J. Batty, Nucl. Phys. A 579 (1994) 518.
4. E. Friedman, A. Gal, J. Mareš, A. Cieplý, Phys. Rev. C 60 (1999) 024314.
5. J. Mareš, E. Friedman, A. Gal, Nucl. Phys. A 770 (2006) 84.
6. J. Schaffner-Bielich, V. Koch, M. Effenberger, Nucl. Phys. A 669 (2000) 153.
7. A. Ramos, E. Oset, Nucl. Phys. A 671 (2000) 481.
8. A. Cieplý, E. Friedman, A. Gal, J. Mareš, Nucl. Phys. A 696 (2001) 173.
9. E. Friedman, A. Gal, Phys. Lett. B 459 (1999) 43.
10. E. Friedman, A. Gal, Nucl. Phys. A 658 (1999) 345.
11. A. Baca, C. García-Recio, J. Nieves, Nucl. Phys. A 673 (2000) 335.
12. E. Friedman, A. Gal, in: S. Bianconi, et al. (Eds.), Proc. III Int. DAΦNE Workshop, Frascati Physics Series vol. XVI, LNF, Frascati, 1999, pp. 677-684.
13. Y. Nogami, Phys. Lett. 7 (1963) 288.
14. T. Yamazaki, Y. Akaishi, Phys. Lett. B 535 (2002) 70.
15. N.V. Shevchenko, A. Gal, J. Mareš, submitted for publication, arXiv:nucl-th/0610022.
16. T. Kishimoto, Phys. Rev. Lett. 83 (1999) 4701.
17. Y. Akaishi, T. Yamazaki, in: S. Bianconi, et al. (Eds.), Proc. III Int. DAΦNE Workshop, Frascati Physics Series vol. XVI, LNF, Frascati, 1999, pp. 59-74.
18. Y. Akaishi, T. Yamazaki, Phys. Rev. C 65 (2002) 044005.
19. S. Wycech, Nucl. Phys. A 450 (1986) 399c.
20. M. Iwasaki, et al., nucl-ex/0310018; T. Suzuki, et al., Nucl. Phys. A 754 (2005) 375c.
21. T. Suzuki, et al., Phys. Lett. B 597 (2004) 263.
22. M. Iwasaki, plenary talk at HYP06, Mainz, October 2006.
23. T. Kishimoto, et al., Nucl. Phys. A 754 (2005) 383c.
24. T. Kishimoto, private communication, September 2006.
25. M. Agnello, et al., Phys. Rev. Lett. 94 (2005) 212303.
26. V.K. Magas, E. Oset, A. Ramos, H. Toki, Phys. Rev. C 74 (2006) 025206.
27. M. Agnello, et al., Nucl. Phys. A 775 (2006) 35.
28. T. Bressani, presented at HYP06, Mainz, October 2006.
29. T. Nagae, plenary talk at HYP06, Mainz, October 2006.
30. S. Piano, presented at HYP06, Mainz, October 2006.
31. J. Mareš, E. Friedman, A. Gal, Phys. Lett. B 606 (2005) 295.
32. T. Waas, M. Rho, W. Weise, Nucl. Phys. A 617 (1997) 449, and references therein.
33. T. Waas, N. Kaiser, W. Weise, Phys. Lett. B 379 (1996) 34.
34. E.G. Drukarev, private communication, May 2006.
35. J. Schaffner, A. Gal, I.N. Mishustin, H. Stöcker, et al., Phys. Lett. B 334 (1994) 268.
36. G.E. Brown, M. Rho, Nucl. Phys. A 596 (1996) 503.
37. W. Scheinast, et al., Phys. Rev. Lett. 96 (2006) 072301, and references therein.
38. M.M. Sharma, M.A. Nagarajan, P. Ring, Phys. Lett. B 312 (1993) 377.
39. Y. Sugahara, H. Toki, Nucl. Phys. A 579 (1994) 557.
40. A. Doté, H. Horiuchi, Y. Akaishi, T. Yamazaki, Phys. Lett. B 590 (2004) 51.
41. A. Doté, H. Horiuchi, Y. Akaishi, T. Yamazaki, Phys. Rev. C 70 (2004) 044313.